Available online at www.sciencedirect.com

SCIENCE DIRECT

European Journal of Mechanics A/Solids 25 (2006) 199–214

An illustration of the equivalence of the loss of ellipticity conditions in spatial and material settings of hyperelasticity

Ellen Kuhl [a], Harm Askes [b], Paul Steinmann [a,*]

[a] University of Kaiserslautern, Faculty of Mechanical Engineering, P.O. Box 3049, D-67653 Kaiserslautern, Germany
[b] Department of Civil and Structural Engineering, University of Sheffield, Sheffield S1 3JD, United Kingdom

Received 24 June 2004; accepted 29 July 2005

Available online 20 October 2005

Abstract

The loss of ellipticity indicated through the rank-one-convexity condition is elaborated for the spatial and material motion problem of continuum mechanics. While the spatial motion problem is characterized through the classical equilibrium equations parametrised in terms of the deformation gradient, the material motion problem is driven by the inverse deformation gradient. As such, it deals with material forces of configurational mechanics that are energetically conjugated to variations of material placements at fixed spatial points. The duality between the two problems is highlighted in terms of balance laws, linearizations including the consistent tangent operators, and the acoustic tensors. Issues of rank-one-convexity are discussed in both settings. In particular, it is demonstrated that if the rank-one-convexity condition is violated, the loss of well-posedness of the governing equations occurs simultaneously in the spatial and in the material motion context. Thus, the material motion problem, i.e. the configurational force balance, does not lead to additional requirements to ensure ellipticity. This duality of the spatial and the material motion approach is illustrated for the hyperelastic case in general and exemplified analytically and numerically for a hyperelastic material of Neo-Hookean type. Special emphasis is dedicated to the geometrical representation of the ellipticity condition in both settings.

Keywords: Loss of ellipticity; Rank-one-convexity; Localization; Configurational mechanics; Spatial and material settings

1. Introduction

Continuum motion can be described via a Lagrangian or a Eulerian description. In the former, material particles are followed in space, whereas in the latter, material flow along fixed spatial positions is tracked. This is closely related to spatial and material settings of continuum mechanics. In the spatial setting, spatial (or physical) forces are dealt with that are energetically conjugated to spatial variations of fixed material points. This is the viewpoint of classical, Newtonian mechanics. Conversely, in the material setting, material (or configurational) forces are encountered that are energetically conjugated to material variations at fixed spatial positions. The latter formalism is also known as the viewpoint due to Eshelby, see Eshelby (1951, 1975). The material setting of continuum mechanics or rather

* Corresponding author.
E-mail addresses: ekuhl@rhrk.uni-kl.de (E. Kuhl), h.askes@sheffield.ac.uk (H. Askes), ps@rhrk.uni-kl.de (P. Steinmann).
URL: http://mechanik.mv.uni-kl.de (P. Steinmann).

0997-7538/$ – see front matter
doi:10.1016/j.euromechsol.2005.07.008

configurational mechanics has received considerable attention in recent years, cf. Chadwick (1975), Maugin and Trimarco (1992), Maugin (1999a, 1999b), Gurtin (1995), Gurtin and Podio-Guidugli (1996), Dascalu and Maugin (1995), Silhavý (1997), Kienzler and Herrmann (2000), Podio-Guidugli (2002) or the extended monographs (Maugin, 1993, 1995; Gurtin, 2000). In particular, the duality between the spatial and the material setting is elucidated for various cases and applications in Maugin (1993), Steinmann (2002a, 2002b, 2002c), Kuhl and Steinmann (2003).

In the context of configurational mechanics, material force residuals arise as a result of inhomogeneities. Thus, the study of the material motion problem is relevant for problems involving propagating discontinuities such as cracks, voids and inclusions. Especially when the two problems, i.e. spatial motion and material motion, are studied in parallel, it is enlighting to analyse the ellipticity of either problem, see e.g. Ball (1977a, 1977b). In the infinitesimal context, the convexity condition is strongly related to the classical criterion of uniqueness in terms of the positive definiteness of the second order work (Drucker, 1950; Hill, 1958). The general convexity condition, however, is typically too restrictive from a physical point of view and moreover too difficult to evaluate from a mathematical point of view. A weaker condition, yet having a well-established mathematical status is the condition of rank-one-convexity. In the infinitesimal sense, rank-one-convexity corresponds to the classical Legendre–Hadamard condition which dates back to the early work of Hadamard on the propagation of waves, see e.g. Hadamard (1903), Hill (1958, 1962), Truesdell and Noll (1965), Ogden (1984). For the class of non-transient problems considered herein, the loss of rank-one-convexity is one-to-one related to the loss of ellipticity which is typically accompanied by the loss of well-posedness of the governing equations. The elaboration of the ellipticity condition is thus of fundamental interest, not only for the spatial but also for the material motion problem.

Although the notions of convexity, uniqueness, monotony, stability, rank-one-convexity, ellipticity and well-posedness are well-established in the spatial motion context, see e.g. Rice (1976), Rice and Rudnicki (1980), Benallal (1992), Benallal and Comi (1996), Benallal and Bigoni (2004), Bigoni (2000), Petryk (1992, 2000) amongst others, the appropriate classification within what we shall call the material motion context has not been considered to the same extend. As an exception the relations between the spatial and material motion convexity and rank-one-convexity condition have been elaborated in a completely different spirit within the framework of functional analysis in Ball (1977b). Here we want to illustrate those rather abstract results within the spatial and material settings of hyperelasticity in order to highlight the connection of these fundamental results to the notion of configurational mechanics. In particular, a difference between the two settings in this respect would be significant, for instance if the material motion problem would lose ellipticity or rather rank-one-convexity at an earlier stage of loading than the spatial motion problem, or vice versa. Recall, that aspects of uniqueness, monotony or convexity can either be studied on the global/structural level or on the local/constitutive level. Within this study, we restrict ourselves to the constitutive level.

After reiterating the governing equations in both settings in Section 2, relevant tangent operators are derived through a consistent linearisation of both problems in Section 3. Next, in Section 4, we elaborate the issue of ellipticity which can be expressed in terms of the acoustic tensors. For illustration purposes, the corresponding localisation analysis is exemplified in Section 5 for a Neo-Hookean material, whereby the eigenvalues of both acoustic tensors are analysed. Finally, some conclusions will be drawn in Section 6. For the sake of completeness, we shall reiterate the classical Legendre–Hadamard condition in Appendix A.

2. Governing equations

To set the stage, let us briefly summarise the relevant kinematic relations, the underlying variational principle and its linearisation and the corresponding stress measures of the spatial and the material motion problem.

2.1. Spatial motion problem

The familiar spatial motion problem is characterised through the nonlinear spatial deformation map $\boldsymbol{x} = \boldsymbol{\varphi}(\boldsymbol{X}, t) : \mathcal{B}_0 \to \mathcal{B}_t$ mapping placements from the material configuration $\mathcal{B}_0$ to the spatial configuration $\mathcal{B}_t$. The corresponding linear tangent map from the material tangent space $T\mathcal{B}_0$ to the spatial tangent space $T\mathcal{B}_t$ can then be expressed in terms of the spatial motion deformation gradient $\boldsymbol{F} = \nabla_X \boldsymbol{\varphi}(\boldsymbol{X}, t) : T\mathcal{B}_0 \to T\mathcal{B}_t$ and its determinant $J = \det \boldsymbol{F} > 0$ which is required to be strictly positive. Moreover, the right and left spatial motion Cauchy–Green strain tensors $\boldsymbol{C} = \boldsymbol{F}^{\mathrm{t}} \cdot \boldsymbol{F}$ and $\boldsymbol{b} = \boldsymbol{F} \cdot \boldsymbol{F}^{\mathrm{t}}$ can be introduced as typical strain measures of the spatial motion problem.

Recall that $\boldsymbol{C}$ can be interpreted as the pull back of the covariant spatial metric whereas $\boldsymbol{b}$ is the push forward of the contravariant material metric. In what follows, we shall restrict ourselves to hyperelastic conservative systems which can essentially be characterised through a variational principle of Dirichlet type. We thus introduce the internal potential energies W_0 and W_t, in this case the strain energy densities per unit volume in $\mathcal{B}_0$ and $\mathcal{B}_t$, respectively. For the sake of simplicity, we shall assume that the external potential energy vanishes identically such that the total energy $\mathcal{I}$ can be introduced as the integral of either of the strain energies density over the corresponding domain.

$$\mathcal{I}(\boldsymbol{\varphi}) = \int_{\mathcal{B}_0} W_0 \,\mathrm{d}V_0 = \int_{\mathcal{B}_t} W_t \,\mathrm{d}V_t \to \text{stat.} \tag{1}$$

Its stationary point obviously corresponds to a vanishing variation of the total energy density $\mathcal{I}$ with respect to the spatial deformation $\boldsymbol{\varphi}$.

$$\delta_{\boldsymbol{\varphi}}\mathcal{I}(\boldsymbol{\varphi}) = \int_{\mathcal{B}_0} \nabla_{\boldsymbol{X}}\delta\boldsymbol{\varphi} : \mathrm{D}_{\boldsymbol{F}} W_0 \,\mathrm{d}V_0 = \int_{\mathcal{B}_t} \nabla_{\boldsymbol{x}}\delta\boldsymbol{\varphi} : [W_t \boldsymbol{I} - \boldsymbol{f}^{\mathrm{t}} \cdot \mathrm{d}_{\boldsymbol{f}} W_t] \,\mathrm{d}V_t = 0. \tag{2}$$

Herein, $\boldsymbol{f}$ denotes the deformation gradient of the material motion problem, which will be discussed in detail later in the following subsection. Moreover, we could formally introduce the linearisation of the above spatial variation $\delta_{\boldsymbol{\varphi}}\mathcal{I}$ with respect to the spatial motion deformation $\boldsymbol{\varphi}$.

$$\Delta_{\boldsymbol{\varphi}}\delta_{\boldsymbol{\varphi}}\mathcal{I}(\boldsymbol{\varphi}) = \int_{\mathcal{B}_0} \nabla_{\boldsymbol{X}}\delta\boldsymbol{\varphi} : \mathrm{D}^2_{\boldsymbol{F}\boldsymbol{F}} W_0 : \nabla_{\boldsymbol{X}}\Delta\boldsymbol{\varphi} \,\mathrm{d}V_0. \tag{3}$$

The particular format of Eq. (2) motivates the introduction of the spatial motion stresses $\boldsymbol{\Pi}^{\mathrm{t}}$ and $\boldsymbol{\sigma}^{\mathrm{t}} = j\boldsymbol{\Pi}^{\mathrm{t}} \cdot \boldsymbol{F}^{\mathrm{t}}$,

$$\boldsymbol{\Pi}^{\mathrm{t}} = \mathrm{D}_{\boldsymbol{F}} W_0, \qquad \boldsymbol{\sigma}^{\mathrm{t}} = W_t \boldsymbol{I} - \boldsymbol{f}^{\mathrm{t}} \cdot \mathrm{d}_{\boldsymbol{f}} W_t \tag{4}$$

whereby the former denotes the classical two-point Piola stress tensor while the latter is typically referred to as Cauchy stress. With these abbreviations at hand, the familiar Euler–Lagrange field equations of the spatial motion problem

$$\mathrm{div}_{\boldsymbol{X}}\, \boldsymbol{\Pi}^{\mathrm{t}} = \boldsymbol{0}, \qquad \mathrm{div}_{\boldsymbol{x}}\, \boldsymbol{\sigma}^{\mathrm{t}} = \boldsymbol{0} \tag{5}$$

follow directly form the evaluation of the spatial variation of the total potential energy (2). For further reference, it proves convenient to additionally introduce the following stress tensors.

$$\boldsymbol{\tau}^{\mathrm{t}} = \boldsymbol{\Pi}^{\mathrm{t}} \cdot \boldsymbol{F}^{\mathrm{t}}, \quad \boldsymbol{M}^{\mathrm{t}} = \boldsymbol{F}^{\mathrm{t}} \cdot \boldsymbol{\Pi}^{\mathrm{t}}, \quad \boldsymbol{Y}^{\mathrm{t}} = \boldsymbol{F}^{\mathrm{t}} \cdot \boldsymbol{\Pi}^{\mathrm{t}} \cdot \boldsymbol{F}^{\mathrm{t}}. \tag{6}$$

Hereby, $\boldsymbol{\tau}^{\mathrm{t}} = J\boldsymbol{\sigma}^{\mathrm{t}}$ denotes the Kirchhoff stress tensor which is typically given in spatial description, $\boldsymbol{M}^{\mathrm{t}}$ is the classical Mandel stress tensor in material description and $\boldsymbol{Y}^{\mathrm{t}}$ is another two-point stress tensor of the spatial motion problem.

2.2. Material motion problem

The material motion problem is the appropriate setting of configurational mechanics. Thereby, in analogy to the spatial motion map $\boldsymbol{\varphi}$, we could introduce a material motion map $\boldsymbol{X} = \boldsymbol{\Phi}(\boldsymbol{x}, t) : \mathcal{B}_t \to \mathcal{B}_0$ which essentially defines the mapping of placements from the spatial configuration $\mathcal{B}_t$ to the material configuration $\mathcal{B}_0$. Accordingly, the material motion deformation gradient $\boldsymbol{f} = \nabla_{\boldsymbol{x}}\boldsymbol{\Phi}(\boldsymbol{x}, t) : T\mathcal{B}_t \to T\mathcal{B}_0$ defines the linear tangent map from the spatial tangent space $T\mathcal{B}_t$ to the material tangent space $T\mathcal{B}_0$, whereby $j = \det \boldsymbol{f} > 0$ denotes the corresponding Jacobian. Moreover, we introduce the right and left material motion Cauchy–Green strain tensors $\boldsymbol{c} = \boldsymbol{f}^{\mathrm{t}} \cdot \boldsymbol{f}$ and $\boldsymbol{B} = \boldsymbol{f} \cdot \boldsymbol{f}^{\mathrm{t}}$ which can be interpreted as the push forward of the covariant material metric and as the pull back of the contravariant spatial metric, respectively. In the case of configurational equilibrium, the Euler–Lagrange equations of the material motion problem follow from the appropriate evaluation of the related Dirichlet principle in terms of the stationarity of the total energy $\mathcal{I}$, however, now parametrised in terms of the material motion map $\boldsymbol{\Phi}$.

$$\mathcal{I}(\boldsymbol{\Phi}) = \int_{\mathcal{B}_t} W_t \,\mathrm{d}V_t = \int_{\mathcal{B}_0} W_0 \,\mathrm{d}V_0 \to \text{stat.} \tag{7}$$

Accordingly, for the material motion problem, the minimum of the total energy density $\mathcal{I}$ corresponds to a vanishing variation with respect to the material deformation $\boldsymbol{\Phi}$.

$$\delta_{\boldsymbol{\Phi}}\mathcal{I}(\boldsymbol{\Phi}) = \int_{\mathcal{B}_t} \nabla_{\boldsymbol{x}}\delta\boldsymbol{\Phi} : \mathrm{d}_{\boldsymbol{f}} W_t \,\mathrm{d}V_t = \int_{\mathcal{B}_0} \nabla_{\boldsymbol{X}}\delta\boldsymbol{\Phi} : [W_0\boldsymbol{I} - \boldsymbol{F}^{\mathrm{t}} \cdot \mathrm{D}_{\boldsymbol{F}} W_0]\,\mathrm{d}V_0 = 0. \tag{8}$$

Again, we could formally introduce the linearisation of the material variation $\delta_{\boldsymbol{\Phi}}\mathcal{I}$ with respect to the material deformation $\boldsymbol{\Phi}$.

$$\Delta_{\boldsymbol{\Phi}}\delta_{\boldsymbol{\Phi}}\mathcal{I}(\boldsymbol{\Phi}) = \int_{\mathcal{B}_t} \nabla_{\boldsymbol{x}}\delta\boldsymbol{\Phi} : \mathrm{d}^2_{\boldsymbol{f}\boldsymbol{f}} W_t : \nabla_{\boldsymbol{x}}\Delta\boldsymbol{\Phi}\,\mathrm{d}V_t. \tag{9}$$

Next, we introduce the material motion stresses $\boldsymbol{\pi}^{\mathrm{t}}$ and $\boldsymbol{\Sigma}^{\mathrm{t}} = J\boldsymbol{\pi}^{\mathrm{t}} \cdot \boldsymbol{f}^{\mathrm{t}}$,

$$\boldsymbol{\pi}^{\mathrm{t}} = \mathrm{d}_{\boldsymbol{f}} W_t, \qquad \boldsymbol{\Sigma}^{\mathrm{t}} = W_0\boldsymbol{I} - \boldsymbol{F}^{\mathrm{t}} \cdot \mathrm{D}_{\boldsymbol{F}} W_0 \tag{10}$$

the former denoting a two-point stress tensor of Piola type and the latter being the classical Eshelby stress, a stress tensor in material description. Accordingly, the Euler–Lagrange field equations of the material motion problem which follow straightforwardly from Eq. (8)

$$\mathrm{div}_{\boldsymbol{x}}\boldsymbol{\pi}^{\mathrm{t}} = \boldsymbol{0}, \qquad \mathrm{div}_{\boldsymbol{X}}\,\boldsymbol{\Sigma}^{\mathrm{t}} = \boldsymbol{0} \tag{11}$$

take a formally dual structure to the Euler–Lagrange equations of the spatial motion problem, compare Eqs. (5). Moreover, it proves convenient to introduce the following stress tensors of the material motion problem,

$$\boldsymbol{\mathcal{T}}^{\mathrm{t}} = \boldsymbol{\pi}^{\mathrm{t}} \cdot \boldsymbol{f}^{\mathrm{t}}, \quad \boldsymbol{m}^{\mathrm{t}} = \boldsymbol{f}^{\mathrm{t}} \cdot \boldsymbol{\pi}^{\mathrm{t}}, \quad \boldsymbol{y}^{\mathrm{t}} = \boldsymbol{f}^{\mathrm{t}} \cdot \boldsymbol{\pi}^{\mathrm{t}} \cdot \boldsymbol{f}^{\mathrm{t}} \tag{12}$$

whereby $\boldsymbol{\mathcal{T}}^{\mathrm{t}} = j\boldsymbol{\Sigma}^{\mathrm{t}}$ denotes a stress measure of Kirchhoff type in material description, $\boldsymbol{m}^{\mathrm{t}}$ is typically addressed as the stress tensor of the chemical potential in spatial description and $\boldsymbol{y}^{\mathrm{t}}$ denotes another two-point stress of the material motion problem.

2.3. Spatial vs. material motion stresses

Obviously, the spatial and the material motion problem are related through the identity map in $\mathcal{B}_0$ as $\mathbf{id}_{\mathcal{B}_0} = \boldsymbol{\Phi}(\boldsymbol{\varphi}(\boldsymbol{X},t),t)$ and in $\mathcal{B}_t$ as $\mathbf{id}_{\mathcal{B}_t} = \boldsymbol{\varphi}(\boldsymbol{\Phi}(\boldsymbol{x},t),t)$, such that the spatial and the material deformation gradient are simply inverses of one another, i.e. $\boldsymbol{f} = \boldsymbol{F}^{-1}$ and $\boldsymbol{F} = \boldsymbol{f}^{-1}$, compare Fig. 1. Accordingly, the spatial Cauchy–Green tensors $\boldsymbol{C}$ and $\boldsymbol{b}$ are also related to their material motion counterparts $\boldsymbol{B}$ and $\boldsymbol{c}$ via their inverses as $\boldsymbol{C}^{-1} = \boldsymbol{B}$ and $\boldsymbol{b}^{-1} = \boldsymbol{c}$. Recall that scalar- or tensor-valued quantities with material reference $\{\bullet\}_0 = J\{\bullet\}_t$ and corresponding quantities with spatial reference $\{\bullet\}_t = j\{\bullet\}_0$ are related via the Piola transforms in terms of the Jacobians J and j. Moreover, material surface flux terms $\{\square\} = J\{\Diamond\} \cdot \boldsymbol{f}^t$ are related to their spatial counterparts $\{\Diamond\} = j\{\square\} \cdot \boldsymbol{F}^t$ through the well-known Nanson's formula. For the hyperelastic case considered herein, we can set up the following useful relations between the spatial stress measures $\boldsymbol{\Pi}^{\mathrm{t}}$, $\boldsymbol{\tau}^{\mathrm{t}}$, $\boldsymbol{M}^{\mathrm{t}}$ and $\boldsymbol{Y}^{\mathrm{t}}$ and the material stress measures $\boldsymbol{\pi}^{\mathrm{t}}$, $\boldsymbol{\mathcal{T}}^{\mathrm{t}}$, $\boldsymbol{m}^{\mathrm{t}}$ and $\boldsymbol{y}^{\mathrm{t}}$ as introduced in Eqs. (6) and (12)

$$\begin{aligned} \boldsymbol{\Pi}^{\mathrm{t}} &= W_0\boldsymbol{f}^{\mathrm{t}} - J\boldsymbol{y}^{\mathrm{t}}, & \boldsymbol{\tau}^{\mathrm{t}} &= W_0\boldsymbol{I} - J\boldsymbol{m}^{\mathrm{t}}, \\ \boldsymbol{M}^{\mathrm{t}} &= W_0\boldsymbol{I} - J\boldsymbol{\mathcal{T}}^{\mathrm{t}}, & \boldsymbol{Y}^{\mathrm{t}} &= W_0\boldsymbol{F}^{\mathrm{t}} - J\boldsymbol{\pi}^{\mathrm{t}} \end{aligned} \tag{13}$$

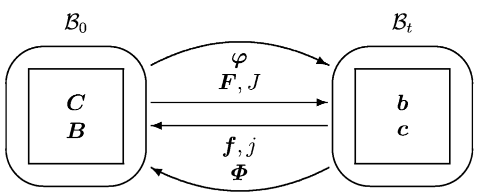

Fig. 1. Spatial vs. material kinematics.

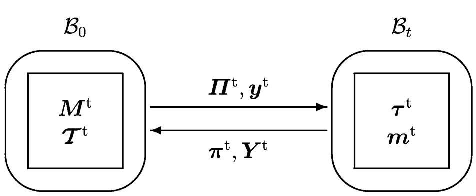

Fig. 2. Spatial vs. material stresses.

and vice versa

$$\begin{aligned} \boldsymbol{\pi}^{\mathrm{t}} &= W_t \boldsymbol{F}^{\mathrm{t}} - j\boldsymbol{Y}^{\mathrm{t}}, \qquad & \boldsymbol{\mathcal{T}}^{\mathrm{t}} &= W_t \boldsymbol{I} - j\boldsymbol{M}^{\mathrm{t}}, \\ \boldsymbol{m}^{\mathrm{t}} &= W_t \boldsymbol{I} - j\boldsymbol{\tau}^{\mathrm{t}}, \qquad & \boldsymbol{y}^{\mathrm{t}} &= W_t \boldsymbol{f}^{\mathrm{t}} - j\boldsymbol{\Pi}^{\mathrm{t}} \end{aligned} \tag{14}$$

by making use of the definitions given in Eqs. (4) and (10), compare Fig. 2.

3. Linearization

The present section is dedicated to the appropriate linearization of the stress strain relations of both, the spatial and the material motion problem. They lend themselves to the introduction or several fourth order tangent operators. Useful relations between spatial and material motion tangent operators will be derived.

3.1. Spatial motion problem

The fourth order tensor A denotes the familiar spatial motion tangent operator in two-point description, i.e. the second derivative of the internal potential energy density W_0 with respect to the spatial motion deformation gradient $\boldsymbol{F}$ as introduced earlier in Eq. (3).

$$\mathsf{A} = \mathrm{D}^2_{\boldsymbol{F}\boldsymbol{F}} W_0 = \mathrm{D}_{\boldsymbol{F}} \boldsymbol{\Pi}^{\mathrm{t}}. \tag{15}$$

For a particular free energy function W_0, e.g. the hyperelastic Neo-Hookean free energy to be elaborated in Section 5, we can express the tangent operator A in terms of the derivatives of the Jacobians J and j

$$\mathrm{D}_{\boldsymbol{F}} J = J\boldsymbol{f}^{\mathrm{t}}, \qquad \mathrm{D}_{\boldsymbol{F}} j = -j\boldsymbol{f}^{\mathrm{t}} \tag{16}$$

and of the derivatives of the deformation gradients $\boldsymbol{F}$ and $\boldsymbol{f}$

$$\mathrm{D}_{\boldsymbol{F}} \boldsymbol{F} = \boldsymbol{I} \,\overline{\otimes}\, \boldsymbol{I}, \quad \mathrm{D}_{\boldsymbol{F}} \boldsymbol{F}^{\mathrm{t}} = \boldsymbol{I} \,\underline{\otimes}\, \boldsymbol{I}, \quad \mathrm{D}_{\boldsymbol{F}} \boldsymbol{f} = -\boldsymbol{f} \,\overline{\otimes}\, \boldsymbol{f}^{\mathrm{t}}, \quad \mathrm{D}_{\boldsymbol{F}} \boldsymbol{f}^{\mathrm{t}} = -\boldsymbol{f}^{\mathrm{t}} \,\underline{\otimes}\, \boldsymbol{f} \tag{17}$$

with respect to the spatial motion deformation gradient $\boldsymbol{F}$ itself. In the above equations, we have introduced the abbreviations $[\bullet \,\overline{\otimes}\, \circ]_{\mathrm{ijkl}} = [\bullet]_{\mathrm{ik}} \otimes [\circ]_{\mathrm{jl}}$ and $[\bullet \,\underline{\otimes}\, \circ]_{\mathrm{ijkl}} = [\bullet]_{\mathrm{il}} \otimes [\circ]_{\mathrm{jk}}$ for the non-standard dyadic products of two second order tensors. With these considerations at hand, we can straightforwardly introduce the pull back and push forward of the two-point tensor A. To this end, we make use of the following operation

$$[\bullet^{\mathrm{t}} \,\overline{\otimes}\, \circ] : \mathsf{A} : [\bullet \,\overline{\otimes}\, \circ^{\mathrm{t}}] \quad \text{with } [\bullet], [\circ] \in \{\boldsymbol{I}, \boldsymbol{F}\} \tag{18}$$

whereby the choice of first tensor $[\bullet] = \boldsymbol{F}$ corresponds to a covariant pull back of the first and third index of A and $[\circ] = \boldsymbol{F}$ denotes a contravariant push forward of the second and fourth index. Obviously, for $[\bullet] = \boldsymbol{I}$ and $[\circ] = \boldsymbol{I}$ the corresponding indices remain unaffected. With the above considerations, we can easily generate the pull back and push forward of the spatial motion tangent operator A.

$$\begin{aligned} \mathsf{b} &= [\boldsymbol{I}^{\mathrm{t}} \,\overline{\otimes}\, \boldsymbol{F}] : \mathsf{A} : [\boldsymbol{I} \,\overline{\otimes}\, \boldsymbol{F}^{\mathrm{t}}], \\ \mathsf{C} &= [\boldsymbol{F}^{\mathrm{t}} \,\overline{\otimes}\, \boldsymbol{I}] : \mathsf{A} : [\boldsymbol{F} \,\overline{\otimes}\, \boldsymbol{I}^{\mathrm{t}}], \\ \mathsf{d} &= [\boldsymbol{F}^{\mathrm{t}} \,\overline{\otimes}\, \boldsymbol{F}] : \mathsf{A} : [\boldsymbol{F} \,\overline{\otimes}\, \boldsymbol{F}^{\mathrm{t}}]. \end{aligned} \tag{19}$$

Accordingly, the fourth order tensor b is expressed in the spatial description similar to the left Cauchy–Green strain tensor $\boldsymbol{b}$ while the fourth order tensor C is denoted in the material description according to the right Cauchy–Green strain tensor $\boldsymbol{C}$. The fourth order tangent operator d is denoted in the two-point description, however, with pairwise opposite indices compared to A, compare Fig. 3.

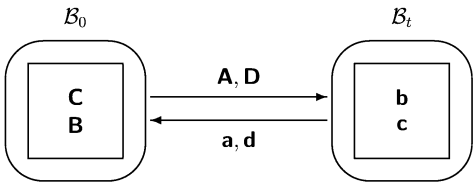

Fig. 3. Spatial vs. material tangent operators.

3.2. Material motion problem

The, to our knowledge up to now never considered, fourth order tangent operator $\mathbf{a}$ of the configurational problem is a tensor in two-point description, characterising the second derivative of the internal potential energy density W_t with respect to the material motion deformation gradient $\boldsymbol{f}$ which was introduced earlier in Eq. (9).

$$\mathbf{a} = \mathrm{d}^2_{\boldsymbol{f}\boldsymbol{f}} W_t = \mathrm{d}_{\boldsymbol{f}} \boldsymbol{\pi}^{\mathrm{t}}. \tag{20}$$

In Section 5, we will evaluate the above equation for a particular hyperelastic free energy function $W_t(\boldsymbol{f})$ of Neo-Hooke type. To this end, we will require the derivatives of the Jacobians j and J

$$\mathrm{d}_{\boldsymbol{f}} j = j \boldsymbol{F}^{\mathrm{t}}, \qquad \mathrm{d}_{\boldsymbol{f}} J = -J \boldsymbol{F}^{\mathrm{t}} \tag{21}$$

and of the deformation gradients $\boldsymbol{f}$ and $\boldsymbol{F}$

$$\mathrm{d}_{\boldsymbol{f}} \boldsymbol{f} = \boldsymbol{I} \overline{\otimes} \boldsymbol{I}, \quad \mathrm{d}_{\boldsymbol{f}} \boldsymbol{f}^{\mathrm{t}} = \boldsymbol{I} \underline{\otimes} \boldsymbol{I}, \quad \mathrm{d}_{\boldsymbol{f}} \boldsymbol{F} = -\boldsymbol{F} \overline{\otimes} \boldsymbol{F}^{\mathrm{t}}, \quad \mathrm{d}_{\boldsymbol{f}} \boldsymbol{F}^{\mathrm{t}} = -\boldsymbol{F}^{\mathrm{t}} \underline{\otimes} \boldsymbol{F} \tag{22}$$

with respect to the material motion deformation gradient $\boldsymbol{f}$. Based on these preliminary considerations, we can introduce the following push forward and pull back operations

$$[\bullet^{\mathrm{t}} \overline{\otimes} \circ] : \mathbf{a} : [\bullet \overline{\otimes} \circ^{\mathrm{t}}] \quad \text{with } [\bullet], [\circ] \in \{\boldsymbol{I}, \boldsymbol{f}\} \tag{23}$$

whereby now $[\bullet] = \boldsymbol{f}$ denotes the covariant push forward of the first and third index of $\mathbf{a}$ and $[\circ] = \boldsymbol{f}$ indicates the contravariant pull back of its second and fourth index, respectively. Again, the identity maps $[\bullet] = \boldsymbol{I}$ and $[\circ] = \boldsymbol{I}$ do not change the corresponding index. We thus introduce the following abbreviations for the material motion tangent operators,

$$\begin{aligned} \mathbf{B} &= [\boldsymbol{I}^{\mathrm{t}} \overline{\otimes} \boldsymbol{f}] : \mathbf{a} : [\boldsymbol{I} \overline{\otimes} \boldsymbol{f}^{\mathrm{t}}], \\ \mathbf{c} &= [\boldsymbol{f}^{\mathrm{t}} \overline{\otimes} \boldsymbol{I}] : \mathbf{a} : [\boldsymbol{f} \overline{\otimes} \boldsymbol{I}^{\mathrm{t}}], \\ \mathbf{D} &= [\boldsymbol{f}^{\mathrm{t}} \overline{\otimes} \boldsymbol{f}] : \mathbf{a} : [\boldsymbol{f} \overline{\otimes} \boldsymbol{f}^{\mathrm{t}}] \end{aligned} \tag{24}$$

whereby $\mathbf{B}$ is obviously a fourth order tensor in material description, $\mathbf{c}$ is denoted in spatial description and $\mathbf{D}$ is a tensor in two-point description similar to the spatial motion tangent operator $\mathbf{A}$ with pairwise opposite indices as $\mathbf{a}$.

3.3. Spatial vs. material tangent operators

In the previous section, we have set up relations between the different spatial and material stress measures. By making use of Eqs. (13) and (14) in particular, we can rewrite the spatial motion tangent operator $\mathbf{A}$ in terms of the material stress $\boldsymbol{\pi}^{\mathrm{t}}$ whereas the material motion tangent operator $\mathbf{a}$ can be expressed in terms of the spatial stress $\boldsymbol{\Pi}^{\mathrm{t}}$.

$$\begin{aligned} \mathbf{A} &= \mathrm{D}_{\boldsymbol{F}} \boldsymbol{\Pi}^{\mathrm{t}} = \mathrm{D}_{\boldsymbol{F}} [J W_t \boldsymbol{f}^{\mathrm{t}} - J \boldsymbol{f}^{\mathrm{t}} \cdot \boldsymbol{\pi}^{\mathrm{t}} \cdot \boldsymbol{f}^{\mathrm{t}}], \\ \mathbf{a} &= \mathrm{d}_{\boldsymbol{f}} \boldsymbol{\pi}^{\mathrm{t}} = \mathrm{d}_{\boldsymbol{f}} [j W_0 \boldsymbol{F}^{\mathrm{t}} - j \boldsymbol{F}^{\mathrm{t}} \cdot \boldsymbol{\Pi}^{\mathrm{t}} \cdot \boldsymbol{F}^{\mathrm{t}}]. \end{aligned} \tag{25}$$

The thorough evaluation of the above equation renders as a new result the following useful relations between the spatial motion tangent operators $\mathbf{A}$, $\mathbf{b}$, $\mathbf{C}$ and $\mathbf{d}$ and their material counterparts $\mathbf{a}$, $\mathbf{B}$, $\mathbf{c}$ and $\mathbf{D}$

$$\begin{aligned} \mathbf{A} &= \boldsymbol{\Pi}^{\mathrm{t}} \otimes \boldsymbol{f}^{\mathrm{t}} - \boldsymbol{f}^{\mathrm{t}} \underline{\otimes} \boldsymbol{\Pi} - \boldsymbol{\Pi}^{\mathrm{t}} \underline{\otimes} \boldsymbol{f} + \boldsymbol{f}^{\mathrm{t}} \otimes \boldsymbol{\Pi}^{\mathrm{t}} - W_0 \boldsymbol{f}^{\mathrm{t}} \otimes \boldsymbol{f}^{\mathrm{t}} + W_0 \boldsymbol{f}^{\mathrm{t}} \underline{\otimes} \boldsymbol{f} + J \mathbf{D}, \\ \mathbf{b} &= \boldsymbol{\tau}^{\mathrm{t}} \otimes \boldsymbol{I} - \boldsymbol{I} \underline{\otimes} \boldsymbol{\tau} - \boldsymbol{\tau}^{\mathrm{t}} \underline{\otimes} \boldsymbol{I} + \boldsymbol{I} \otimes \boldsymbol{\tau}^{\mathrm{t}} - W_0 \boldsymbol{I} \otimes \boldsymbol{I} + W_0 \boldsymbol{I} \underline{\otimes} \boldsymbol{I} + J \mathbf{c}, \\ \mathbf{C} &= \boldsymbol{M}^{\mathrm{t}} \otimes \boldsymbol{I} - \boldsymbol{I} \underline{\otimes} \boldsymbol{M} - \boldsymbol{M}^{\mathrm{t}} \underline{\otimes} \boldsymbol{I} + \boldsymbol{I} \otimes \boldsymbol{M}^{\mathrm{t}} - W_0 \boldsymbol{I} \otimes \boldsymbol{I} + W_0 \boldsymbol{I} \underline{\otimes} \boldsymbol{I} + J \mathbf{B}, \\ \mathbf{d} &= \boldsymbol{Y}^{\mathrm{t}} \otimes \boldsymbol{F}^{\mathrm{t}} - \boldsymbol{F}^{\mathrm{t}} \underline{\otimes} \boldsymbol{Y} - \boldsymbol{Y}^{\mathrm{t}} \underline{\otimes} \boldsymbol{F} + \boldsymbol{F}^{\mathrm{t}} \otimes \boldsymbol{Y}^{\mathrm{t}} - W_0 \boldsymbol{F}^{\mathrm{t}} \otimes \boldsymbol{F}^{\mathrm{t}} + W_0 \boldsymbol{F}^{\mathrm{t}} \underline{\otimes} \boldsymbol{F} + J \mathbf{a} \end{aligned} \tag{26}$$

and vice versa,

$$\begin{aligned} \mathbf{a} &= \boldsymbol{\pi}^{\mathrm{t}} \otimes \boldsymbol{F}^{\mathrm{t}} - \boldsymbol{F}^{\mathrm{t}} \underline{\otimes} \boldsymbol{\pi} - \boldsymbol{\pi}^{\mathrm{t}} \underline{\otimes} \boldsymbol{F} + \boldsymbol{F}^{\mathrm{t}} \otimes \boldsymbol{\pi}^{\mathrm{t}} - W_t \boldsymbol{F}^{\mathrm{t}} \otimes \boldsymbol{F}^{\mathrm{t}} + W_t \boldsymbol{F}^{\mathrm{t}} \underline{\otimes} \boldsymbol{F} + j \mathbf{d}, \\ \mathbf{B} &= \boldsymbol{\mathcal{T}}^{\mathrm{t}} \otimes \boldsymbol{I} - \boldsymbol{I} \underline{\otimes} \boldsymbol{\mathcal{T}} - \boldsymbol{\mathcal{T}}^{\mathrm{t}} \underline{\otimes} \boldsymbol{I} + \boldsymbol{I} \otimes \boldsymbol{\mathcal{T}}^{\mathrm{t}} - W_t \boldsymbol{I} \otimes \boldsymbol{I} + W_t \boldsymbol{I} \underline{\otimes} \boldsymbol{I} + j \mathbf{C}, \\ \mathbf{c} &= \boldsymbol{m}^{\mathrm{t}} \otimes \boldsymbol{I} - \boldsymbol{I} \underline{\otimes} \boldsymbol{m} - \boldsymbol{m}^{\mathrm{t}} \underline{\otimes} \boldsymbol{I} + \boldsymbol{I} \otimes \boldsymbol{m}^{\mathrm{t}} - W_t \boldsymbol{I} \otimes \boldsymbol{I} + W_t \boldsymbol{I} \underline{\otimes} \boldsymbol{I} + j \mathbf{b}, \\ \mathbf{D} &= \boldsymbol{y}^{\mathrm{t}} \otimes \boldsymbol{f}^{\mathrm{t}} - \boldsymbol{f}^{\mathrm{t}} \underline{\otimes} \boldsymbol{y} - \boldsymbol{y}^{\mathrm{t}} \underline{\otimes} \boldsymbol{f} + \boldsymbol{f}^{\mathrm{t}} \otimes \boldsymbol{y}^{\mathrm{t}} - W_t \boldsymbol{f}^{\mathrm{t}} \otimes \boldsymbol{f}^{\mathrm{t}} + W_t \boldsymbol{f}^{\mathrm{t}} \underline{\otimes} \boldsymbol{f} + j \mathbf{A} \end{aligned} \tag{27}$$

compare Fig. 3. Recall the practical relevance of the fourth order tangent operators within a Newton–Raphson based solution strategy in a finite element scheme. In this context, the tangent operators $\mathbf{A}$ and $\mathbf{a}$ are of particular importance, see Kuhl et al. (2004) and Askes et al. (2004). Their relevance in the context of rank-one-convexity is illustrated in the following section.

4. Ellipticity

In the previous section, we have introduced the spatial and the material tangent operators A and a. Their positive semi-definiteness is typically analysed to study the convexity of the underlying motion problem. In what follows, we shall relax the classical condition of convexity to the in some cases less restrictive requirement of rank-one-convexity. Following arguments of duality, we discuss the rank-one-convexity condition or rather ellipticity condition for both the spatial and the material motion problem. By setting up relations between the spatial and the material motion acoustic tensor, we will show that both are simply related via weighted pull back/push forward operations. A relation to the classical Legendre–Hadamard condition in terms of the acoustic tensors is given in Appendix A.

4.1. Spatial motion problem

The rank-one-convexity condition of the spatial motion problem can be expressed as follows.

$$[\boldsymbol{m} \otimes \boldsymbol{N}] : \mathsf{A} : [\boldsymbol{m} \otimes \boldsymbol{N}] \geqslant 0. \tag{28}$$

For $[\boldsymbol{m} \otimes \boldsymbol{N}] : \mathsf{A} : [\boldsymbol{m} \otimes \boldsymbol{N}] > 0$, it ensures that the underlying quasi-static spatial motion problem remains elliptic. By introducing the contravariant pull back of the spatial unit tangent $\boldsymbol{m}$ and the covariant push forward of the material unit normal $\boldsymbol{N}$ as

$$\overline{\boldsymbol{M}} = \boldsymbol{f} \cdot \boldsymbol{m} = \boldsymbol{m} \cdot \boldsymbol{f}^{\mathrm{t}}, \qquad \bar{\boldsymbol{n}} = \boldsymbol{f}^{\mathrm{t}} \cdot \boldsymbol{N} = \boldsymbol{N} \cdot \boldsymbol{f} \tag{29}$$

we can reformulate the above equation in terms of the four different tangent operators A, b, C and d introduced in Eq. (19).

$$\begin{aligned} [\boldsymbol{m} \otimes \bar{\boldsymbol{n}}] : \mathsf{b} : [\boldsymbol{m} \otimes \bar{\boldsymbol{n}}] &\geqslant 0, \\ [\overline{\boldsymbol{M}} \otimes \boldsymbol{N}] : \mathsf{C} : [\overline{\boldsymbol{M}} \otimes \boldsymbol{N}] &\geqslant 0, \\ [\overline{\boldsymbol{M}} \otimes \bar{\boldsymbol{n}}] : \mathsf{d} : [\overline{\boldsymbol{M}} \otimes \bar{\boldsymbol{n}}] &\geqslant 0. \end{aligned} \tag{30}$$

Alternatively, the above equations could be formulated as a requirement of positive semi-definiteness

$$\begin{aligned} \boldsymbol{m} \cdot \boldsymbol{q} \cdot \boldsymbol{m} &\geqslant 0, \qquad & \boldsymbol{q} &= [\boldsymbol{I} \otimes \boldsymbol{N}] : \mathsf{A} \cdot \boldsymbol{N} = [\boldsymbol{I} \otimes \bar{\boldsymbol{n}}] : \mathsf{b} \cdot \bar{\boldsymbol{n}}, \\ \overline{\boldsymbol{M}} \cdot \overline{\boldsymbol{Q}} \cdot \overline{\boldsymbol{M}} &\geqslant 0, \qquad & \overline{\boldsymbol{Q}} &= [\boldsymbol{I} \otimes \boldsymbol{N}] : \mathsf{C} \cdot \boldsymbol{N} = [\boldsymbol{I} \otimes \bar{\boldsymbol{n}}] : \mathsf{d} \cdot \bar{\boldsymbol{n}} \end{aligned} \tag{31}$$

in terms of the second order tensor $\boldsymbol{q}$ in spatial description and its pull back $\overline{\boldsymbol{Q}} = \boldsymbol{F}^{\mathrm{t}} \cdot \boldsymbol{q} \cdot \boldsymbol{F}$ in material description, a condition which can equivalently be expressed in the following form.

$$\det(\boldsymbol{q}) \geqslant 0, \qquad \det(\overline{\boldsymbol{Q}}) \geqslant 0. \tag{32}$$

Because of its connection with the propagation of infinitesimal plane waves, the second order tensor $\boldsymbol{q}$ is called the acoustic tensor of the spatial motion problem. The vector $\boldsymbol{N}$ then represents the direction of wave propagation which corresponds to the normal to the discontinuity surface in the quasi-static case while $\boldsymbol{m}$ takes the interpretation of a jump vector.

4.2. Material motion problem

In complete analogy to the spatial motion problem, in configurational mechanics, the rank-one-convexity condition of the material motion problem takes the following format.

$$[\boldsymbol{M} \otimes \boldsymbol{n}] : \mathsf{a} : [\boldsymbol{M} \otimes \boldsymbol{n}] \geqslant 0. \tag{33}$$

For $[\boldsymbol{M} \otimes \boldsymbol{n}] : \mathsf{a} : [\boldsymbol{M} \otimes \boldsymbol{n}] > 0$, the above rank-one-convexity condition yields to the condition of ellipticity of the quasi-static material motion problem. With the help of the contravariant push forward of the material tangent $\boldsymbol{M}$ and the covariant pull back of the spatial normal $\boldsymbol{n}$

$$\overline{\boldsymbol{m}} = \boldsymbol{F} \cdot \boldsymbol{M} = \boldsymbol{M} \cdot \boldsymbol{F}^{\mathrm{t}}, \qquad \bar{\boldsymbol{N}} = \boldsymbol{F}^{\mathrm{t}} \cdot \boldsymbol{n} = \boldsymbol{n} \cdot \boldsymbol{F} \tag{34}$$

we can easily generate alternative expressions in terms of the different tangent operators a, B, c and D introduced in Eq. (24).

$$\begin{aligned}[\boldsymbol{M} \otimes \overline{\boldsymbol{N}}] : \mathsf{B} : [\boldsymbol{M} \otimes \overline{\boldsymbol{N}}] &\geqslant 0, \\ [\overline{\boldsymbol{m}} \otimes \boldsymbol{n}] : \mathsf{c} : [\overline{\boldsymbol{m}} \otimes \boldsymbol{n}] &\geqslant 0, \\ [\overline{\boldsymbol{m}} \otimes \overline{\boldsymbol{N}}] : \mathsf{D} : [\overline{\boldsymbol{m}} \otimes \overline{\boldsymbol{N}}] &\geqslant 0.\end{aligned} \tag{35}$$

A reformulation of the above equations

$$\begin{aligned}\boldsymbol{M} \cdot \boldsymbol{Q} \cdot \boldsymbol{M} &\geqslant 0, \qquad & \boldsymbol{Q} &= [\boldsymbol{I} \otimes \boldsymbol{n}] : \mathsf{a} \cdot \boldsymbol{n} = [\boldsymbol{I} \otimes \overline{\boldsymbol{N}}] : \mathsf{B} \cdot \overline{\boldsymbol{N}}, \\ \overline{\boldsymbol{m}} \cdot \bar{\boldsymbol{q}} \cdot \overline{\boldsymbol{m}} &\geqslant 0, & \bar{\boldsymbol{q}} &= [\boldsymbol{I} \otimes \boldsymbol{n}] : \mathsf{c} \cdot \boldsymbol{n} = [\boldsymbol{I} \otimes \overline{\boldsymbol{N}}] : \mathsf{D} \cdot \overline{\boldsymbol{N}}\end{aligned} \tag{36}$$

introduces the requirement of positive semi-definiteness of the material motion acoustic tensor $\boldsymbol{Q}$ and its push forward $\bar{\boldsymbol{q}} = \boldsymbol{f}^{\mathrm{t}} \cdot \boldsymbol{Q} \cdot \boldsymbol{f}$, whereby their non-negative determinant

$$\det(\boldsymbol{Q}) \geqslant 0, \qquad \det(\bar{\boldsymbol{q}}) \geqslant 0 \tag{37}$$

ensures ellipticity of the material motion problem. Again, $\boldsymbol{n}$ characterises the spatial normal to the discontinuity surface while $\boldsymbol{M}$ denotes the corresponding jump vector.

4.3. Spatial vs. material acoustic tensor

To elaborate the relations between the spatial motion acoustic tensor $\boldsymbol{q} = [\boldsymbol{I} \otimes \boldsymbol{N}] : \mathrm{D}_{\boldsymbol{F}} \boldsymbol{\Pi} \cdot \boldsymbol{N}$ and its material motion counterpart $\boldsymbol{Q} = [\boldsymbol{I} \otimes \boldsymbol{n}] : \mathrm{d}_{\boldsymbol{f}} \boldsymbol{\pi} \cdot \boldsymbol{n}$ we shall express $\mathrm{D}_{\boldsymbol{F}} \boldsymbol{\Pi}$ and $\mathrm{d}_{\boldsymbol{f}} \boldsymbol{\pi}$ in terms of their dual counterparts according to Eqs. (26) and (27).

$$\begin{aligned}\boldsymbol{q} &= \boldsymbol{t} \otimes \bar{\boldsymbol{n}} - \bar{\boldsymbol{n}} \otimes \boldsymbol{t} - W_0 \bar{\boldsymbol{n}} \otimes \bar{\boldsymbol{n}} + W_0 \bar{\boldsymbol{n}} \otimes \bar{\boldsymbol{n}} - \boldsymbol{t} \otimes \bar{\boldsymbol{n}} + \bar{\boldsymbol{n}} \otimes \boldsymbol{t} + J \boldsymbol{f}^{\mathrm{t}} \cdot \bar{\boldsymbol{n}} \cdot \mathrm{d}_{\boldsymbol{f}} \boldsymbol{\pi} \cdot \bar{\boldsymbol{n}} \cdot \boldsymbol{f}, \\ \boldsymbol{Q} &= \boldsymbol{T} \otimes \overline{\boldsymbol{N}} - \overline{\boldsymbol{N}} \otimes \boldsymbol{T} - W_t \overline{\boldsymbol{N}} \otimes \overline{\boldsymbol{N}} + W_t \overline{\boldsymbol{N}} \otimes \overline{\boldsymbol{N}} - \boldsymbol{T} \otimes \overline{\boldsymbol{N}} + \overline{\boldsymbol{N}} \otimes \boldsymbol{T} + j \boldsymbol{F}^{\mathrm{t}} \cdot \overline{\boldsymbol{N}} \cdot \mathrm{D}_{\boldsymbol{F}} \boldsymbol{\Pi} \cdot \overline{\boldsymbol{N}} \cdot \boldsymbol{F}.\end{aligned} \tag{38}$$

For notational simplicity, we have introduced the spatial and the material traction vector $\boldsymbol{t} = \boldsymbol{\Pi}^{\mathrm{t}} \cdot \boldsymbol{N}$ and $\boldsymbol{T} = \boldsymbol{\pi}^{\mathrm{t}} \cdot \boldsymbol{n}$, the push forward of the material normal $\bar{\boldsymbol{n}}$ and the pull back of the spatial normal $\overline{\boldsymbol{N}}$. Due to the symmetric structure of the acoustic tensors, all but the last term cancel and we are left with the following remarkably simple expressions.

$$\begin{aligned}\boldsymbol{q} &= [\boldsymbol{I} \otimes \boldsymbol{N}] : \mathrm{D}_{\boldsymbol{F}} \boldsymbol{\Pi} \cdot \boldsymbol{N} = J \boldsymbol{f}^{\mathrm{t}} \cdot [\boldsymbol{I} \otimes \bar{\boldsymbol{n}}] : \mathrm{d}_{\boldsymbol{f}} \boldsymbol{\pi} \cdot \bar{\boldsymbol{n}} \cdot \boldsymbol{f}, \\ \boldsymbol{Q} &= [\boldsymbol{I} \otimes \boldsymbol{n}] : \mathrm{d}_{\boldsymbol{f}} \boldsymbol{\pi} \cdot \boldsymbol{n} = j \boldsymbol{F}^{\mathrm{t}} [\boldsymbol{I} \otimes \overline{\boldsymbol{N}}] : \mathrm{D}_{\boldsymbol{F}} \boldsymbol{\Pi} \cdot \overline{\boldsymbol{N}} \cdot \boldsymbol{F}.\end{aligned} \tag{39}$$

The right-hand sides of the above equation can easily be identified as the scaled push forward of the material motion acoustic tensor $\bar{\boldsymbol{q}}$ and the pull back of the spatial motion acoustic tensor $\overline{\boldsymbol{Q}}$ introduced in Eqs. (36) and (31), compare Fig. 4.

$$\begin{aligned}\boldsymbol{q} &= J \lambda_n^2 \bar{\boldsymbol{q}}, \\ \boldsymbol{Q} &= j \Lambda_N^2 \overline{\boldsymbol{Q}}\end{aligned} \quad \text{with} \quad \begin{aligned}\bar{\boldsymbol{q}} &= \boldsymbol{f}^{\mathrm{t}} \cdot \boldsymbol{Q} \cdot \boldsymbol{f}, \\ \overline{\boldsymbol{Q}} &= \boldsymbol{F}^{\mathrm{t}} \cdot \boldsymbol{q} \cdot \boldsymbol{F}.\end{aligned} \tag{40}$$

Apparently, the spatial motion acoustic tensor $\boldsymbol{q}$ follows straightforwardly from a push forward of its material motion counterpart $\boldsymbol{Q}$ weighted by the corresponding Jacobian and the square of the related stretch $\lambda_n = \|\bar{\boldsymbol{n}}\| = \sqrt{\boldsymbol{N} \cdot \boldsymbol{B} \cdot \boldsymbol{N}} = \Lambda_N^{-1}$ and $\Lambda_N = \|\overline{\boldsymbol{N}}\| = \sqrt{\boldsymbol{n} \cdot \boldsymbol{b} \cdot \boldsymbol{n}} = \lambda_n^{-1}$. Of course, this result is neither astonishing nor unexpected. The equivalence of the spatial and material rank-one-convexity condition (28) and (33) has been shown already by Ball in the more abstract setting of functional analysis, see Ball (1977b). By making use of the change of variables formula, he proved that $W_t(\boldsymbol{f})$ is rank-one-convex if and only if $W_0(\boldsymbol{F})$ is rank-one-convex without explicitly referring to the implications

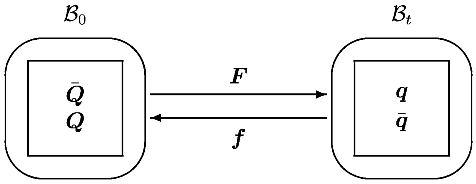

Fig. 4. Spatial vs. material acoustic tensors.

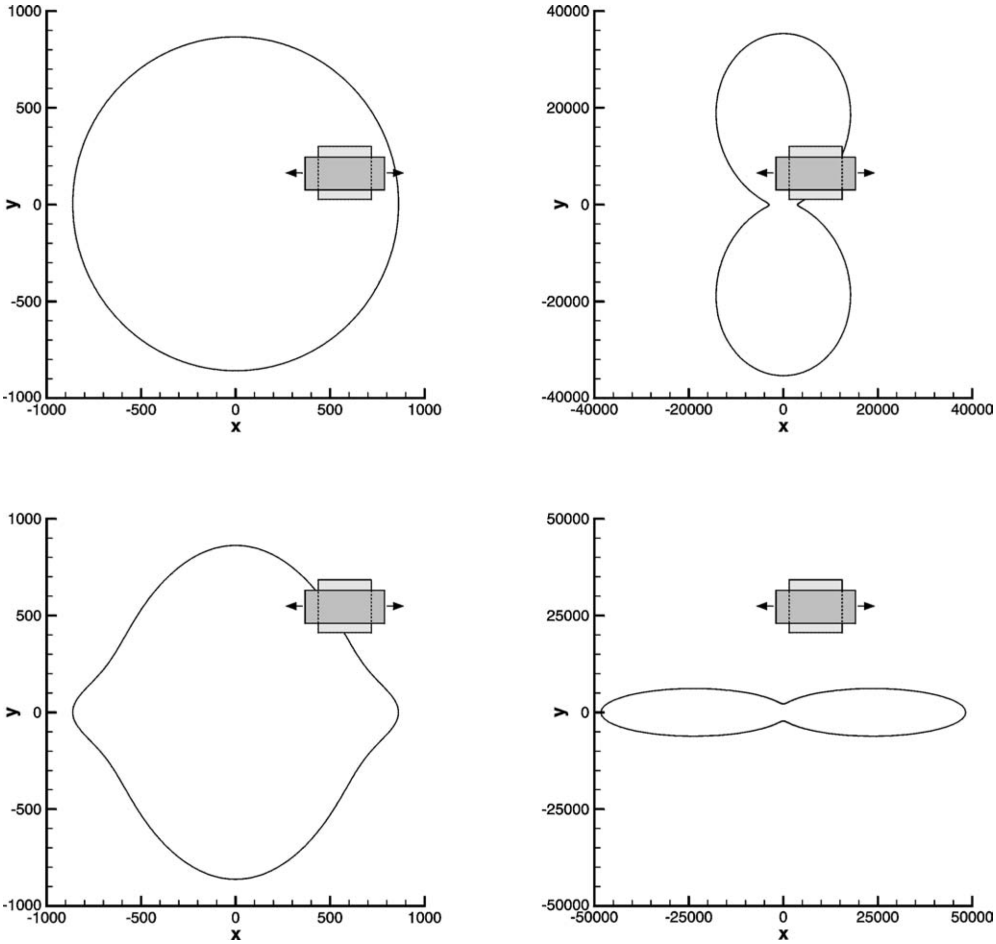

Fig. 5. Pure shear with $\Lambda = 2$ and $\nu = 0.45$—eigenvalues of spatial motion problem (top) and material motion problem (bottom).

within configurational mechanics. Thus, in summary of our investigations, as the main result it occurs that provided that the underlying deformation is invertible, i.e. $J > 0$ and accordingly $j > 0$, $\boldsymbol{F} = \boldsymbol{f}^{-1}$ and $\boldsymbol{f} = \boldsymbol{F}^{-1}$, the loss of ellipticity of the spatial and the material motion problem takes place simultaneously. Accordingly, the determinant of the acoustic tensors $\boldsymbol{q}$ and $\boldsymbol{Q}$

$$\det(\boldsymbol{q}) = 0 \quad \Leftrightarrow \quad \det(\boldsymbol{Q}) = 0 \tag{41}$$

vanishes simultaneously for the spatial and the material motion problem.

5. Model problem: Neo-Hookean material

In the remainder of this study, we assume a frequently used strain energy density of the compressible Neo-Hookean type with

$$W_0 = \frac{1}{2}\lambda_0 \ln^2(J) + \frac{1}{2}\mu_0\big[\boldsymbol{C} : \boldsymbol{I} - n^{\dim} - 2\ln(J)\big] \tag{42}$$

for the spatial and

$$W_t = \frac{1}{2}\lambda_t \ln^2(j^{-1}) + \frac{1}{2}\mu_t\big[\boldsymbol{c}^{-1} : \boldsymbol{I} - n^{\dim} - 2\ln(j^{-1})\big] \tag{43}$$

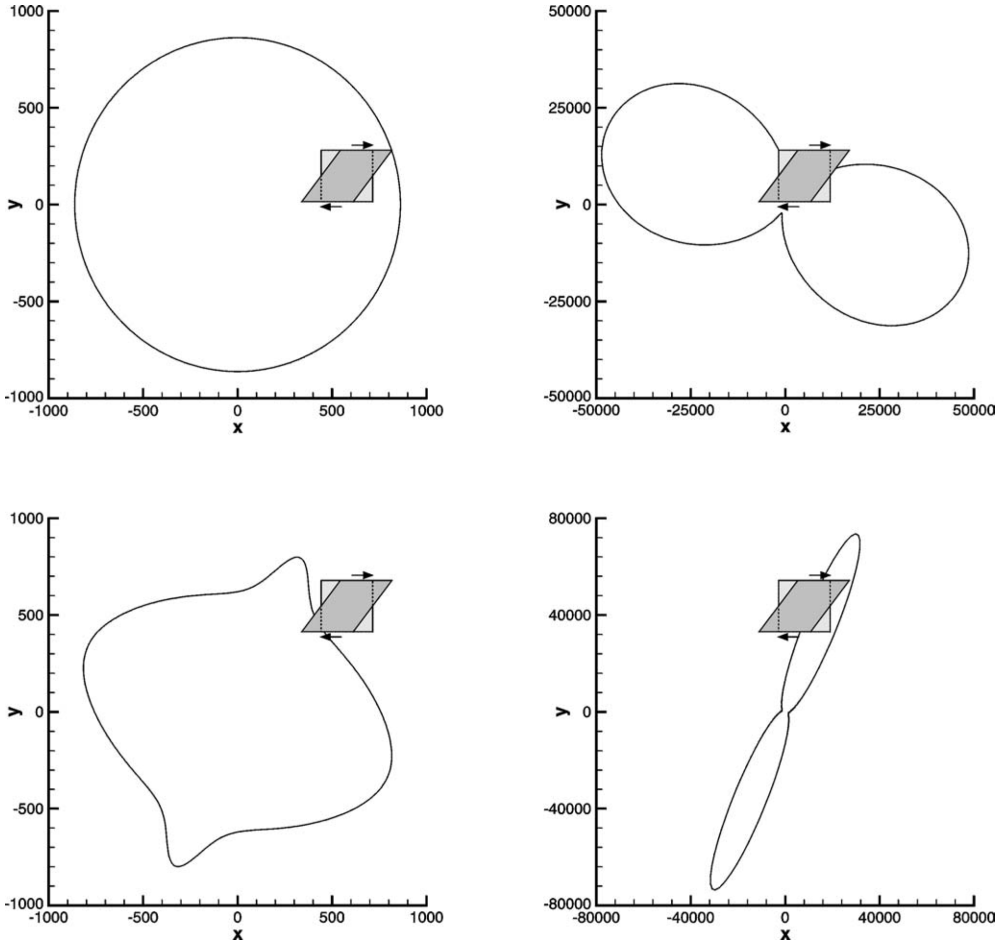

Fig. 6. Simple shear with $\Lambda = 2$ and $\nu = 0.45$—eigenvalues of spatial motion problem (top) and material motion problem (bottom).

for the material motion case. Thereby, $n^{\dim}$ is the number of spatial dimensions of the problem under consideration and μ_0, λ_0, $\mu_t = j\mu_0$ and $\lambda_t = j\lambda_0$ are the Lamé parameters of the spatial and the material motion problem, respectively. With this particularisation, the tangent operator of the spatial motion problem can be elaborated as

$$\tan \mathbf{A} = \lambda_0 \boldsymbol{f}^t \otimes \boldsymbol{f}^t + \mu_0 \boldsymbol{I} \,\overline{\otimes}\, \boldsymbol{I} + \left[\mu_0 - \lambda_0 \ln(J)\right] \boldsymbol{f}^t \,\underline{\otimes}\, \boldsymbol{f} \tag{44}$$

whereas the much more involved tangent operator of the material motion problem can be written as follows.

$$\begin{aligned} \tan \mathbf{a} = {} & \left[W_t - 2\lambda_t \ln(J) + 2\mu_t + \lambda_t\right] \boldsymbol{F}^t \otimes \boldsymbol{F}^t - \left[W_t - \lambda_t \ln(J) + \mu_t\right] \boldsymbol{F}^t \,\underline{\otimes}\, \boldsymbol{F} \\ & + \mu_t [\boldsymbol{C} \cdot \boldsymbol{F}^t \,\underline{\otimes}\, \boldsymbol{F} + \boldsymbol{F}^t \,\underline{\otimes}\, \boldsymbol{F} \cdot \boldsymbol{C} - \boldsymbol{C} \cdot \boldsymbol{F}^t \otimes \boldsymbol{F}^t - \boldsymbol{F}^t \otimes \boldsymbol{C} \cdot \boldsymbol{F}^t + \boldsymbol{C} \,\overline{\otimes}\, \boldsymbol{b}]. \end{aligned} \tag{45}$$

The acoustic tensors that correspond to the spatial and to the material motion problem are obtained by substituting Eqs. (44) and (45) into Eqs. (31) and (36). Although the tangent operators themselves differ considerably for the spatial and the material motion case, the acoustic tensors of the spatial

$$\boldsymbol{q} = \left[\lambda_0\left[1 - \ln(J)\right] + \mu_0\right] \bar{\boldsymbol{n}} \otimes \bar{\boldsymbol{n}} + \mu_0 \boldsymbol{I} \tag{46}$$

and the material motion problem

$$\boldsymbol{Q} = \Lambda_N^2 \left[\left[\lambda_t\left[1 - \ln(J)\right] + \mu_t\right] \boldsymbol{N} \otimes \boldsymbol{N} + \mu_t \boldsymbol{C}\right] \tag{47}$$

take a remarkably similar format and are of course related through Eq. (40).

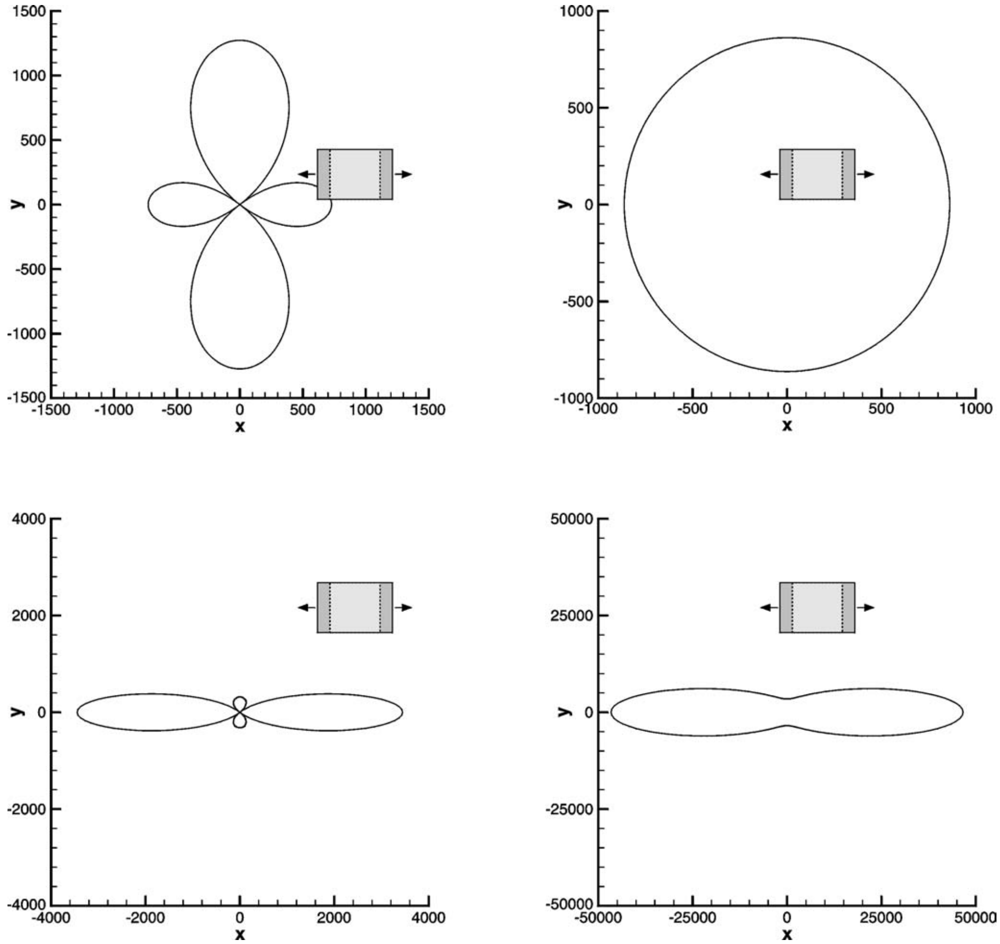

Fig. 7. Uniaxial tension with $\Lambda = 4$ and $\nu = 0.45$—eigenvalues of spatial motion problem (top) and material motion problem (bottom)

5.1. Analytical elaboration of rank-one-convexity

Loss of ellipticity or rather loss of rank-one-convexity occurs when the determinant of the acoustic tensor becomes zero. Following Eqs. (46) and (47), the two determinants for the two-dimensional case can be elaborated in Cartesian coordinates as

$$\det(\boldsymbol{q}) = \left[\lambda_0\mu_0\left[1 - \ln(J)\right] + \mu_0^2\right]\left[[f_{11}c + f_{21}s]^2 + [f_{12}c + f_{22}s]^2\right] + \mu_0^2 \tag{48}$$

and

$$\det(\boldsymbol{Q}) = \Lambda_N\left[\left[\lambda_t\mu_t\left[1 - \ln(J)\right] + \mu_t^2\right]\left[[F_{11}s - F_{12}c]^2 + [F_{21}s - F_{22}c]^2\right] + \mu_t^2 J^2\right] \tag{49}$$

respectively. Herein, we have introduced the short-hand notation $c = \cos(\alpha)$ and $s = \sin(\alpha)$ in terms of the angle α defining the material normal as $\boldsymbol{N} = [\cos\alpha, \sin\alpha]^{\mathrm{t}}$. For a number of fundamental loading cases, we examine when loss of ellipticity occurs:

- Pure shear is described by taking the deformation gradient equal to $F_{11} = \Lambda$, $F_{22} = 1/\Lambda$ and $F_{12} = F_{21} = 0$, hence $J = \det(\boldsymbol{F}) = 1$. It can be verified that Eqs. (48) and (49) then reduce to a summation of quadratic terms. Therefore, ellipticity is a priori guaranteed throughout.
- Simple shear is invoked via $F_{11} = F_{22} = 1$, $F_{12} = \Lambda$ and $F_{21} = 0$. The same observations apply as for the case of pure shear.

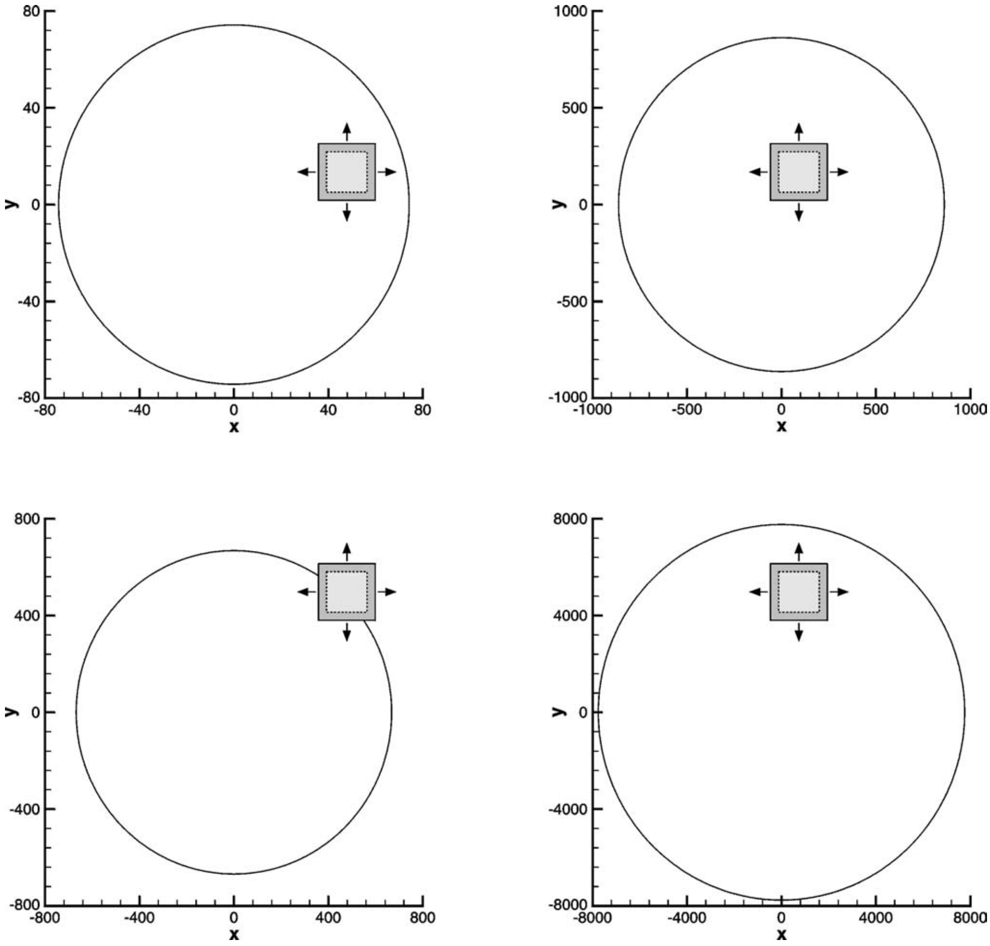

Fig. 8. Biaxial tension with $\Lambda = 3$ and $\nu = 0.45$—eigenvalues of spatial motion problem (top) and material motion problem (bottom).

- Uniaxial tension can be described by $F_{11} = \Lambda$, $F_{22} = 1$ and $F_{12} = F_{21} = 0$. Elaborating either of the two determinants given in Eqs. (48) and (49) reveals that ellipticity is lost if $\lambda_0[1 - \ln(\Lambda)] + 2\mu_0 \leqslant 0$ whereby the critical direction for *both* determinants is given by $\alpha = \pi/2$. From solving the above equation, a critical stretch Λ can be determined in terms of the Poisson's ratio ν. Ellipticity is lost if $\Lambda \geqslant \exp([1 - \nu]/\nu)$.
- Biaxial tension is generated by taking $F_{11} = F_{22} = \Lambda$ and $F_{12} = F_{21} = 0$. Ellipticity is lost if the transcendental inequality $\lambda_0[1 - \ln(\Lambda^2)] + \mu_0[1 + \Lambda^2] \leqslant 0$ is satisfied, where again the two determinants give identical results. For values of $\nu > 0.4464$ ellipticity cannot be guaranteed.

As has been argued already in the previous sections: if loss of ellipticity occurs, it occurs *concurrently* in the spatial motion problem and in the material motion problem.

5.2. Numerical elaboration of rank-one-convexity

Next, the eigenvalues of the two acoustic tensors are investigated. The same four loading cases are studied as in Section 5.1. Throughout, the elastic constants have been taken as $\lambda_0 = 7759$ MPa and $\mu_0 = 862$ MPa corresponding to $E = 2500$ MPa and $\nu = 0.45$ in the small strain limit. For the loading cases pure shear and simple shear a stretch $\Lambda = 2$ has been taken, we analyse the uniaxial tension case with $\Lambda = 4$, and $\Lambda = 3$ has been used for the biaxial case. The results are plotted in Figs. 5–8. For the considered loading cases four eigenvalues are non-trivial: two according to $\boldsymbol{q}$ and two according to $\boldsymbol{Q}$. In Figs. 5–8 the eigenvalues are multiplied with the components of $\boldsymbol{N}$ to arrive at a

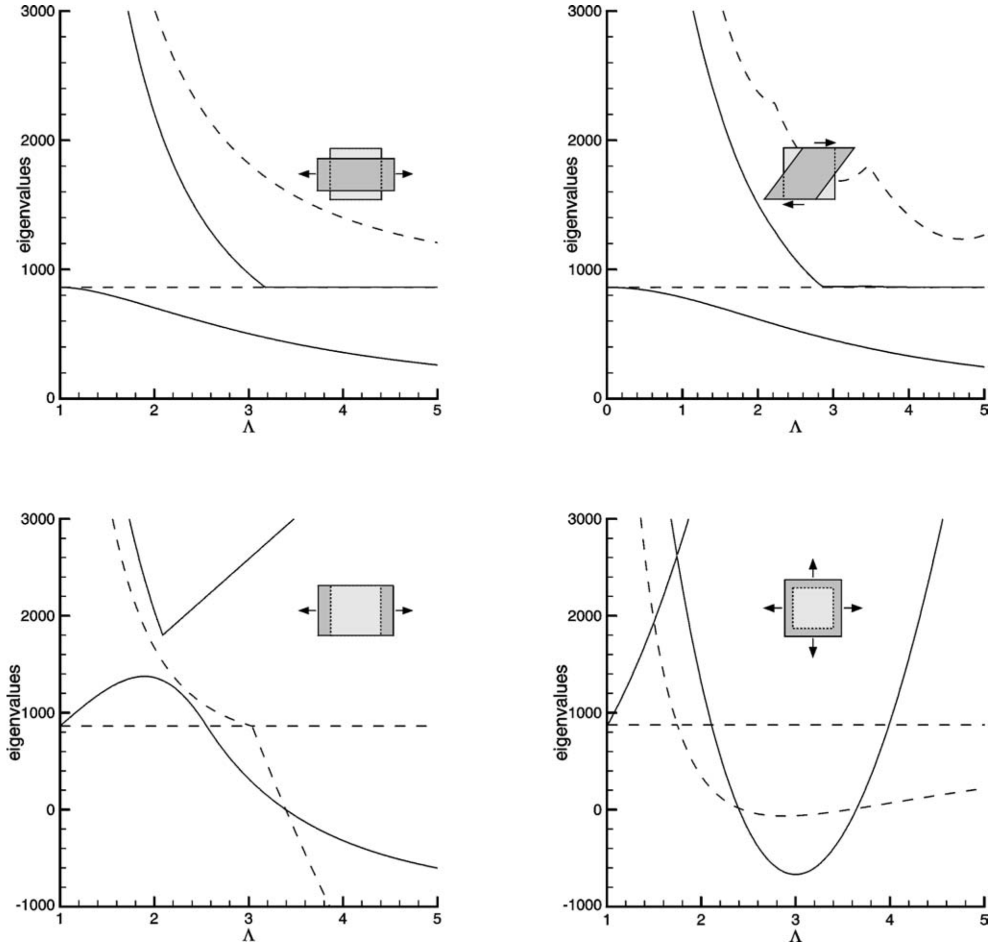

Fig. 9. Eigenvalues as a function of the stretch Λ for the material motion problem (solid) and the spatial motion problem (dashed) — pure shear (top left), simple shear (top right), uniaxial tension (bottom left) and biaxial tension (bottom right).

two-dimensional visualisation: denoting the eigenvalues by h, we plot $h\cos(\alpha)$ on the horizontal axis and $h\sin(\alpha)$ on the vertical axis.

For the cases of pure shear and simple shear, where ellipticity or rather rank-one-convexity is guaranteed for any value of the stretch Λ, the eigenvalues remain always positive. Since the two acoustic tensors $\boldsymbol{q}$ and $\boldsymbol{Q}$ are related via two contractions in terms of the (inverse) deformation gradient, the shape of the eigenvalue plots is very similar for the spatial motion problem as compared to the material motion problem; cf. the top rows and bottom rows in Figs. 5 and 6. For instance, the smaller eigenvalue of the spatial motion problem yields a circle with radius μ_0 (see Figs. 5 and 6, upper left), which translates into lemon-like curves for the material motion problem (Figs. 5 and 6, bottom left). Similar observations hold for the larger eigenvalue, depicted in the right columns of Figs. 5 and 6. In the latter curves, the direction of the maximum eigenvalue for the spatial motion problem coincides with the direction of the minimum eigenvalue for the material motion problem, and vice versa. This is due to the fact that if for a certain angle α a maximum value for $\boldsymbol{F}$ is obtained, then a minimum value for $\boldsymbol{f}$ is found, and vice versa.

If uniaxial tension is assumed, a critical stretch exists beyond which the determinants of the acoustic tensors become negative. In Fig. 7 the eigenvalues of both acoustic tensors are plotted for a stretch larger than the critical stretch. For certain values of α, one of the eigenvalues becomes negative which results in flower-like curves as shown in the left column of Fig. 7. This dependence on α was already used in the derivation of the critical equation $\lambda_0[1 - \ln(\Lambda)] + 2\mu_0 \leqslant 0$. The negative eigenvalues appear and develop in similar ways for the spatial motion problem and the material motion problem. Again, in the spatial motion problem one of the eigenvalues adopts the (non-negative) constant value μ_0, which is transformed into a (non-negative) eigenvalue for the material motion problem via two contractions with the deformation gradient (cf. right column of Fig. 7).

Finally, loss of ellipticity, i.e. rank-one-convexity, can also occur in case of biaxial tension. In contrast to uniaxial tension, loss of rank-one-convexity does not depend on the angle α. This is reflected in the circles plotted in Fig. 8. The left column of Fig. 8 consists of eigenvalues that are all negative, the right column contains only positive eigenvalues. The radii of the circles described by the material motion problem are related to the radii of the circles from the spatial motion problem via a factor Λ^2. According to Eq. (40), the two acoustic tensors relate as $\boldsymbol{Q} = j\Lambda_N^2 \boldsymbol{F}^{\mathrm{t}} \cdot \boldsymbol{q} \cdot \boldsymbol{F}$. For this specific loading case with $\boldsymbol{F} = \Lambda \boldsymbol{I}$ and $j = \Lambda^{-2}$, the above equation simplifies to $\boldsymbol{Q} = \Lambda^2 \boldsymbol{q}$, compare also Eqs. (46) and (47).

In Fig. 9 the evolution of the *minimum* eigenvalues of $\boldsymbol{q}$ and $\boldsymbol{Q}$ is plotted as a function of the stretch Λ. Note that these minimum values do not necessarily correspond to a single orientation α during the entire loading process. It is again seen that the eigenvalues for the loading cases pure shear and simple shear are always positive, and that one of the eigenvalues of the spatial motion problem is constant and equal to the Lamé constant μ_0. For the loading cases uniaxial tension and biaxial tension one of the two eigenvalues for either problem (spatial motion problem or material motion problem) may become negative. The critical values of Λ for which this occurs have been derived analytically in Section 5.1; here, it is confirmed numerically that negative eigenvalues appear simultaneously in the spatial motion problem and the material motion problem.

6. Conclusions

In this paper, we have considered the conditions for ellipticity or rather rank-one-convexity for the common spatial and the material motion problem of configurational mechanics. The governing equations, linearizations and acoustic tensors for the two problems have been presented in a completely dual format. As a consequence from the classical far-reaching result by Ball (1977a) it turns out that the acoustic tensors associated with the two problems can be retrieved from one another via straightforward push forward/pull back operations. Loss of ellipticity or rather rank-one-convexity clearly occurs simultaneously in the spatial and in the material motion problem although the mechanical interpretation of these two problems is quite different. In other words, studying the material motion problem or rather the problems of configurational mechanics does not lead to additional difficulties: as long as the spatial motion problem remains well-posed, the material motion problem will not become ill–posed due to the loss of rank-one-convexity.

This has been illustrated for a hyperelastic sample material with a compressible Neo-Hookean strain energy density. Four fundamental loading cases have been investigated, both analytically and numerically: if negative eigenvalues occur, they appear concurrently in the acoustic tensors of the two problems.

Appendix A. Spatial and material Legendre–Hadamard condition

For the sake of completeness, we shall briefly summarize the traditional derivation of the Legendre–Hadamard condition as illustrated in Hadamard (1903), Thomas (1961) and Hill (1962). Its derivations are based on the kinematic compatibility conditions for a first order discontinuity surface

$$[\![\mathrm{D}_t \boldsymbol{F}]\!] = \omega \boldsymbol{m} \otimes \boldsymbol{N}, \qquad [\![\mathrm{d}_t \boldsymbol{f}]\!] = \Omega \boldsymbol{M} \otimes \boldsymbol{n} \tag{A.1}$$

which are also referred to as Maxwell's compatibility conditions (Maxwell, 1873). Therein, $\boldsymbol{N}$ and $\boldsymbol{n}$ represent the material and the spatial normal to the discontinuity surface, $\boldsymbol{M}$ and $\boldsymbol{m}$ are the corresponding jump vectors and Ω and ω denote the magnitude of the jump as illustrated in Fig. A.1. The evaluation of Cauchy's lemma in combination with Cauchy's theorem then renders the equilibrium equations across a singular surface,

$$[\![\mathrm{D}_t \boldsymbol{\Pi}^{\mathrm{t}}]\!] \cdot \boldsymbol{N} = \boldsymbol{0}, \qquad [\![\mathrm{d}_t \boldsymbol{\pi}^{\mathrm{t}}]\!] \cdot \boldsymbol{n} = \boldsymbol{0} \tag{A.2}$$

whereby $[\![\bullet]\!] = [\bullet]^+ - [\bullet]^-$ denotes the jump of the quantity $[\bullet]$ across the singular surface. Together with incremental constitutive equation for a hyperelastic material for the spatial $\mathrm{D}_t \boldsymbol{\Pi}^{\mathrm{t}} = \mathbf{A} : \mathrm{D}_t \boldsymbol{F}$ and the material motion problem $\mathrm{d}_t \boldsymbol{\pi}^{\mathrm{t}} = \mathbf{a} : \mathrm{d}_t \boldsymbol{f}$ the equilibrium equations (A.2) can be reformulated as follows.

$$[\![\mathbf{A} : \mathrm{D}_t \boldsymbol{F}]\!] \cdot \boldsymbol{N} = \boldsymbol{0}, \qquad [\![\mathbf{a} : \mathrm{d}_t \boldsymbol{f}]\!] \cdot \boldsymbol{n} = \boldsymbol{0}. \tag{A.3}$$

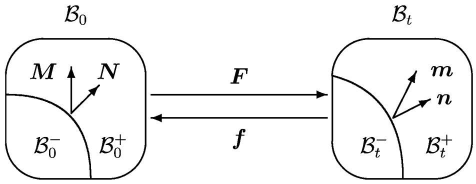

Fig. A.1. Spatial vs. material kinematics of singular surfaces.

Last, we make use of Hill's assumption of a linear comparison solid (Hill, 1958), i.e. $[\![\mathsf{A}]\!] = \mathbf{0}$ and $[\![\mathsf{a}]\!] = \mathbf{0}$, respectively, to end up with alternative representations of Eqs. (28) and (33).

$$\big[\mathsf{A} : [\omega \boldsymbol{m} \otimes \boldsymbol{N}]\big] \cdot \boldsymbol{N} = \mathbf{0}, \qquad \big[\mathsf{a} : [\Omega \boldsymbol{M} \otimes \boldsymbol{n}]\big] \cdot \boldsymbol{n} = \mathbf{0}. \tag{A.4}$$

These can be recast into the corresponding special eigenvalue problems $\boldsymbol{q} \cdot \boldsymbol{m} = \mathbf{0}$ and $\boldsymbol{Q} \cdot \boldsymbol{M} = \mathbf{0}$ in terms of the acoustic tensors of the spatial and the material motion problem $\boldsymbol{q} = [\boldsymbol{I} \otimes \boldsymbol{N}] : \mathrm{D}_{\boldsymbol{F}} \boldsymbol{\Pi} \cdot \boldsymbol{N}$ and $\boldsymbol{Q} = [\boldsymbol{I} \otimes \boldsymbol{n}] : \mathrm{d}_{\boldsymbol{f}} \boldsymbol{\pi} \cdot \boldsymbol{n}$. For the non-transient case considered herein, the vanishing determinant of the acoustic tensors

$$\det(\boldsymbol{q}) = 0, \qquad \det(\boldsymbol{Q}) = 0 \tag{A.5}$$

indicates the loss of ellipticity of the spatial and the material motion problem which manifests itself in the formation of rank-one-laminates. The angles θ and Θ

$$\cos(\theta) = \boldsymbol{m} \cdot \boldsymbol{n}, \qquad \cos(\Theta) = \boldsymbol{M} \cdot \boldsymbol{N} \tag{A.6}$$

between the acoustic axes $\boldsymbol{m}$ and $\boldsymbol{M}$ and the unit normals $\boldsymbol{n}$ and $\boldsymbol{N}$ characterise the corresponding failure mode. Thereby, the spatial unit normal $\boldsymbol{n}$ of the spatial motion problem and the material normal $\boldsymbol{N}$ of the material motion problem can be generated by the corresponding covariant push forward $\bar{\boldsymbol{n}} = \boldsymbol{N} \cdot \boldsymbol{f}$ and pull back $\overline{\boldsymbol{N}} = \boldsymbol{n} \cdot \boldsymbol{F}$. Of course, the mere push forward or pull back of a unit normal does not render vectors of unit length. However, their normalisations $\boldsymbol{n} = \bar{\boldsymbol{n}}/\lambda_n$ and $\boldsymbol{N} = \overline{\boldsymbol{N}}/\Lambda_N$ in terms of the spatial and material stretch λ_n and Λ_N are straightforward. The equivalence of the spatial and the material Legendre–Hadamard conditions (A.4),

$$\big[\mathsf{A} : [\omega \boldsymbol{m} \otimes \boldsymbol{N}]\big] \cdot \boldsymbol{N} = \mathbf{0} \quad \Leftrightarrow \quad \big[\mathsf{a} : [\Omega \boldsymbol{M} \otimes \boldsymbol{n}]\big] \cdot \boldsymbol{n} = \mathbf{0} \tag{A.7}$$

follows straightforwardly from the fundamental result of Eq. (41).

References

Askes, H., Kuhl, E., Steinmann, P., 2004. An ALE formulation based on spatial and material settings of continuum mechanics. Part 2: Classification and applications. Comput. Methods Appl. Mech. Engrg. 193, 4223–4245.

Ball, J.M., 1977a. Convexity conditions and existence theorems in nonlinear elasticity. Arch. Rational Mech. Anal. 63, 337–403.

Ball, J.M., 1977b. Constitutive inequalities and existence theorems in nonlinear elasticity. In: Knops, R.J. (Ed.), Nonlinear Analysis and Mechanics: Heriot–Watt Symposium, vol. 1. Pitman, London, pp. 187–241.

Benallal, A., 1992. On localization phenomena in thermo-elasto-plasticity. Arch. Mech. 44, 15–29.

Benallal, A., Bigoni, D., 2004. Effects of temperature and thermo-mechanical couplings on material instabilities and strain localization of inelastic materials. J. Mech. Phys. Solids 52, 725–753.

Benallal, A., Comi, C., 1996. Localization analysis via a geometrical method. Int. J. Solids Structures 33, 99–119.

Bigoni, D., 2000. Bifurcation and instability of non-associative elastoplastic solids. In: Petryk, H. (Ed.), Material Instabilities in Elastic and Plastic Solids. In: CISM Courses and Lectures, vol. 414. Springer-Verlag, Wien.

Chadwick, P., 1975. Applications of an energy-momentum tensor in non-linear elastostatics. J. Elasticity 5, 249–258.

Dascalu, C., Maugin, G.A., 1995. The thermoelastic material-momentum equation. J. Elasticity 39, 201–212.

Drucker, D.C., 1950. Some implications of work-hardening and ideal plasticity. Quart. Appl. Math. 7, 411–418.

Eshelby, J.D., 1951. The force on an elastic singularity. Philos. Trans. Roy. Soc. London 244, 87–112.

Eshelby, J.D., 1975. The elastic energy-momentum tensor. J. Elasticity 5, 321–335.

Gurtin, M.E., 1995. On the nature of configurational forces. Arch. Rational Mech. Anal. 131, 67–100.

Gurtin, M.E., 2000. Configurational Forces as Basic Concepts of Continuum Physics. Springer-Verlag, New York.

Gurtin, M.E., Podio-Guidugli, P., 1996. On configurational inertial forces at phase interfaces. J. Elasticity 44, 255–269.

Hadamard, J., 1903. Leçons sur la Propagation des Ondes, Librairie Scientifique A. Hermann et Fils, Paris.

Hill, R., 1958. A general theory of uniqueness and stability in elastic-plastic solids. J. Mech. Phys. Solids 6, 236–249.

Hill, R., 1962. Acceleration waves in solids. J. Mech. Phys. Solids 10, 1–16.

Kienzler, R., Herrmann, G., 2000. Mechanics in Material Space with Applications to Defect and Fracture Mechanics. Springer-Verlag, Berlin.

Kuhl, E., Askes, H., Steinmann, P., 2004. An ALE formulation based on spatial and material settings of continuum mechanics. Part 1: Generic hyperelastic formulation. Comput. Methods Appl. Mech. Engrg. 193, 4207–4222.

Kuhl, E., Steinmann, P., 2003. On spatial and material settings of thermo-hyperelastodynamics for open systems. Acta Mech. 160, 179–217.

Maugin, G.A., 1993. Material Inhomogeneities in Elasticity. Chapman & Hall, London.

Maugin, G.A., 1995. Material forces: concepts and applications. Appl. Mech. Rev. 48, 213–245.

Maugin, G.A., 1999a. The Thermomechanics of Nonlinear Irreversible Behaviors. World Scientific.

Maugin, G.A., 1999b. On the universality of the thermomechanics of forces driving singular sets. Arch. Appl. Mech. 69, 1–15.

Maugin, G.A., Trimarco, C., 1992. Pseudomomentum and material forces in nonlinear elasticity: variational formulations and application to brittle fracture. Acta Mech. 94, 1–28.

Maxwell, J.C., 1873. Treatise on Elasticity and Magnetism. Clarendon, Oxford.

Ogden, R.W., 1984. Non-Linear Elastic Deformations. Ellis Horwood, Chichester.

Petryk, H., 1992. Material instability and strain-rate discontinuities in incremental nonlinear continua. J. Mech. Phys. Solids 40, 1227–1250.

Petryk, H., 2000. Theory and material instability in incremental nonlinear plasticity. In: Petryk, H. (Ed.), Material Instabilities in Elastic and Plastic Solids. In: CISM Courses and Lectures, vol. 414. Springer-Verlag, Wien.

Podio-Guidugli, P., 2002. Material forces: are they needed?. Mech. Res. Comm. 29, 513–519.

Rice, J.R., 1976. The localization of plastic deformation. In: Koiter, W. (Ed.), Theoretical and Applied Mechanics. North-Holland, pp. 207–220.

Rice, J.R., Rudnicki, J.W., 1980. A note on some features of the theory of localization of deformation. Int. J. Solids Structures 16, 597–605.

Silhavý, M., 1997. The Mechanics and Thermodynamics of Continuous Media. Springer-Verlag, New York.

Steinmann, P., 2002a. On spatial and material settings of hyperelastodynamics. Acta Mech. 156, 193–218.

Steinmann, P., 2002b. On spatial and material settings of thermo-hyperelastodynamics. J. Elasticity 66, 109–157.

Steinmann, P., 2002c. On spatial and material settings of hyperelastostatic crystal defects. J. Mech. Phys. Solids 50, 1743–1766.

Thomas, T.Y., 1961. Plastic Flow and Fracture in Solids. Academic Press, New York.

Truesdell, C., Noll, W., 1965. The non-linear field theories of mechanics. In: Flügge, S. (Ed.), Handbuch der Physik, vol. III/3. Springer-Verlag, Berlin.